Surface Science 283 (1993) 438–446
North-Holland

surface science

Surface structures and conductance at initial stages in epitaxy of metals on a Si(111) surface

Shuji Hasegawa [a,b] and Shozo Ino [a]

[a] *Department of Physics, Faculty of Science, University of Tokyo, Hongo, Bunkyo-ku, Tokyo 113, Japan*
[b] *PRESTO, Research Development Corporation of Japan (JRDC), Japan*

Received 22 April 1992; accepted for publication 15 July 1992

In situ measurements of surface conductance, combined with simultaneous observations of reflection high-energy electron diffraction, clearly demonstrated strong dependence of the conductance on the substrate–surface structures and epitaxial growth modes at initial stages of metal depositions on a Si(111) surface at room temperature. In the case of Ag deposition onto a Si(111)-$\sqrt{3} \times \sqrt{3}$-Ag surface, the resistance near the surface region showed steep decrease with small Ag coverage, while it scarcely changed for Ag deposition onto a clean 7×7-substrate. In the case of Au depositions onto Si(111)-5×2, $\sqrt{3} \times \sqrt{3}$, and 6×6-Au surfaces, the resistance greatly increased at the beginning, and then decreased during Au deposition. The resistance change for Au deposition onto a clean 7×7-surface was, on the other hand, much smaller at the same coverage region. These dependences of the surface conductance on the substrate–surface structures are understood in terms of the Fermi level pinning and band bending at each surface.

1. Introduction

The electrical properties of semiconductor surfaces have been extensively studied for more than 50 years from industrial as well as scientific interests [1–3]. Their various phenomena are understood in terms of space-charge layers, surface/interface states, Schottky barriers, and others. These also have led to a vast field of physics on two-dimensional electron systems [4]. The atomic structures of the surfaces, on the other hand, have been another major subject for semiconductor surface physics [5,6]. Various kinds of surface science techniques have been employed to investigate the atomic arrangements of clean and foreign-material-adsorbed surfaces. Although, however, considerable progresses have been achieved for the two main subjects, systematic correlations between the electric nature and the atomic structures of surfaces seem as yet only fragmentary.

The Schottky-barrier height at epitaxial $NiSi_2$/Si(111) contacts was found to be strongly influenced by the atomic structure of the interface [7]. Heslinga et al. [8] also demonstrated that the barrier heights of two types of contacts, Si(111)-7×7-Pb and Si(111)-$\sqrt{3} \times \sqrt{3}$-Pb, are quite different. They insist that any theories of Schottky-barrier formation based solely on bulk properties or metal-induced gap states fail to explain the observed difference in barrier height, emphasizing the importance of the local atomic and electronic structures at the interface.

In spite of a great number of studies on the electrical transport characteristics parallel to the surface of clean and metal- or gas-adsorbed semiconductor surfaces [1,2,9–12], understanding on the structure dependence of the characteristics is still only limited. Demuth and Persson employed high-resolution electron-energy-loss spectroscopy to investigate the surface conductivity of a clean and metal-covered Si(111) surface [13,14]. Jałochowski and Bauer measured the electrical resistivity of thin metal films on a Si(111) surface with simultaneous observation of reflection high-energy electron diffraction (RHEED) intensity oscillations, to observe size effects [15].

We carried out recently in situ observations of the changes both in atomic structures and in surface conductance during initial epitaxial growth of metal (Ag and Au) films on a Si(111) surface [16]. While monitoring the structural changes with RHEED during metal depositions, the conductance parallel to the surface was simultaneously measured. The conductance was found to show characteristic changes crucially depending on the substrate–surface structures and epitaxial growth styles of the films. The observed variations in surface conductance changes are tentatively attributed to changes in surface space-charge layers and in the conduction through inhomogeneous metal films. This paper describes systematic investigations of Ag- and Au-induced surface structures, in addition to the results in the previous paper [16], including the result of In adsorption on an Ag-covered Si surface. Interesting phenomena of the conductance changes after closing the metal-evaporator shutter are also reported and discussed relating to adatom migration on the surface.

2. Experimental procedures

The measurements were performed in an ultrahigh vacuum chamber with an ion, a turbomolecular, and a titanium sublimation pump having a base pressure of around 2×10^{-10} Torr and keeping a 10^{-10} Torr range during metal depositions. An n-type Si(111) wafer of 48–50 $\Omega \cdot$cm resistivity and $23 \times 5 \times 0.4$ mm^3 size was mounted on a pair of Ta rods and clamped with Ta plates (fig. 1). Before each measurement run, the surface was cleaned to obtain a clear 7×7 RHEED pattern, by several flash heatings up to 1500 K for 5 s with a direct current of 9.8 A through the Ta rod electrodes, and followed by cooling down after the current was turned off. The conductance of the central portion of the wafer, under isothermal conditions at room temperature (RT), was measured as a voltage drop between a pair of Ta wire contacts (0.4 mm in diameter) ~ 5 mm apart, kept in elastic contact with the wafer, with a constant current of 10 μA supplied through the Ta rod electrodes. The heat treatment for cleaning with the Ta wires in contact made their contact resistance small and steady. A linear relation in the current–voltage characteristics was confirmed in the range from -1 to 1 mA with 0 V at 0 A. It took time from 30 min to 1 h after the surface preparations at high temperatures to attain the isothermal condition at RT and for the resistance to be constant before the metal deposition. The structural changes of the surface between the pair of Ta wire contacts could be simultaneously analyzed with RHEED of 15 kV acceleration. Ag and Au were evaporated with constant rates from alumina-coated W baskets which were placed ~ 50 cm away from the Si substrate. The amount of deposited material, expressed here in units of ML (monolayer, 1 ML = 7.8×10^{14} atoms/cm^2), was monitored with a quartz-crystal oscillator. Since the primary electron beam of ~ 1 μA in RHEED disturbed the voltage between the Ta wire contacts, the beam was always turned off during the measurement, except for the intermittent observations of the RHEED patterns in the course of metal deposition.

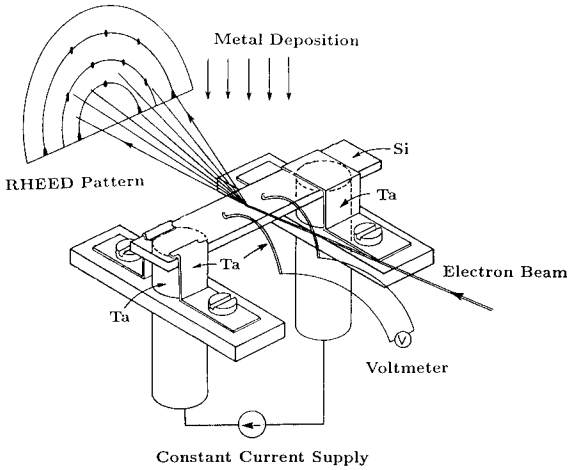

Fig. 1. Sample holder, drawn upside down.

3. Experimental results

3.1. Ag on a Si(111) surface

Fig. 2 shows the surface resistance changes, which are indicated as voltage drops between the Ta wire contacts, during Ag deposition (rate: 0.55 ML/min) at RT onto a clean 7×7 surface (fig. 2a), a $\sqrt{3} \times \sqrt{3}$-Ag surface (fig. 2b), and a 6×1-Ag surface (fig. 2c), respectively. The RHEED patterns observed at the points indicated by arrows in the figure are shown in figs. 2e–2j.

The change in resistance in fig. 2a was very small until the 7×7 pattern disappeared, with the exception of a slight increase just after opening the evaporator shutter. In response to the subsequent development of a texture structure of the Ag film (fig. 2f), the resistance began to decrease steeply. This RHEED pattern indicates that the Ag film grows in a quasi-layer-by-layer fashion, consisting of twining two-dimensional (2D) Ag crystals [17]. In the case of Ag deposition onto the $\sqrt{3} \times \sqrt{3}$ surface (fig. 2b), on the other hand, the phenomenon seems rather different. The resistance measurement was carried out at RT after cooling down from 670 K, at which the $\sqrt{3} \times \sqrt{3}$ structure (fig. 2g) had been prepared on the substrate with 1 ML Ag coverage [18–20]. After an abrupt decrease in the resistance at the beginning (less than 0.1 ML deposition), it decreases at a moderate rate during Ag deposition. In this case, a ring pattern, with some preferential-orientation spots from Ag crystals, gradually emerged in the RHEED pattern with increasing the amount of deposition, while the clear $\sqrt{3} \times \sqrt{3}$ spots remained to the end (fig. 2h). This means that the deposited Ag atoms nucleate in three-dimensional (3D) form on the $\sqrt{3}$ surface and scarcely cover the substrate [21]. This implies high surface diffusivity of Ag adatoms on the $\sqrt{3}$ surface, compared with on the 7×7 surface. An abrupt decrease in the resistance at opening the evaporator shutter and an abrupt increase at the shutter closed suggest an influence of radiation from the Ag evaporator. However, radiation from the same type of empty evaporator, placed near the Ag evaporator, and heated up to the same temperature, scarcely changed the resistance [16]. We can safely say, therefore, that it is the deposited Ag atoms that cause the resistance changes. Then, the steep raise in resistance after closing the evaporator shutter in fig. 2b may correspond to a process of nucleation of Ag adatoms on the $\sqrt{3}$ surface. In the case of deposition onto the 6×1-Ag surface (fig. 2c), surprisingly, the resistance scarcely changed during Ag deposition up to 5.6 ML coverage. The 6×1 structure (fig. 2i) had been created by making $\frac{2}{3}$ ML Ag atoms desorb from the $\sqrt{3} \times \sqrt{3}$-Ag surface at around 870 K, and then by cooling down to RT [17]. Although the pattern showed a 3×1 periodicity at elevated temperatures, the $\frac{1}{6}$-order spots appeared in the course of cooling the wafer down to RT. The 6×1 RHEED pattern was quickly (around 0.2 ML) converted into the 3×1 pattern after the Ag deposition started at RT, and then into the 1×1 structure. The pattern after 5.6 ML Ag deposition (fig. 2j) shows a similar growth style of the Ag film as in the case of 7×7 surface (fig. 2f), but the rotations of the grown Ag crystals around the texture axis are more restricted due to the influence of the underlying 3×1-structural atomic arrangement, and the Ag crystals are more 3D-like.

In this way, crucially depending on the substrate–surface structures, the epitaxial growth styles of room-temperature-deposited Ag films as well as the surface conductance changes are quite different.

During In deposition at RT, in place of Ag, onto the Si(111)-$\sqrt{3} \times \sqrt{3}$-Ag surface (fig. 2d), the resistance change was completely different from that in fig. 2b. After steep increase in resistance at the initial stage of In deposition, it almost remained constant in spite of increase in In coverage. The $\sqrt{3} \times \sqrt{3}$-Ag structure was destroyed to convert into the 1×1 RHEED pattern at around 1.5 ML In coverage. This result should be distinctly contrasted with the case of Ag deposition onto the same $\sqrt{3} \times \sqrt{3}$-Ag surface in fig. 2b. The In adatoms on the $\sqrt{3}$-Ag surface seem to electrically act in a manner opposite to Ag adatoms.

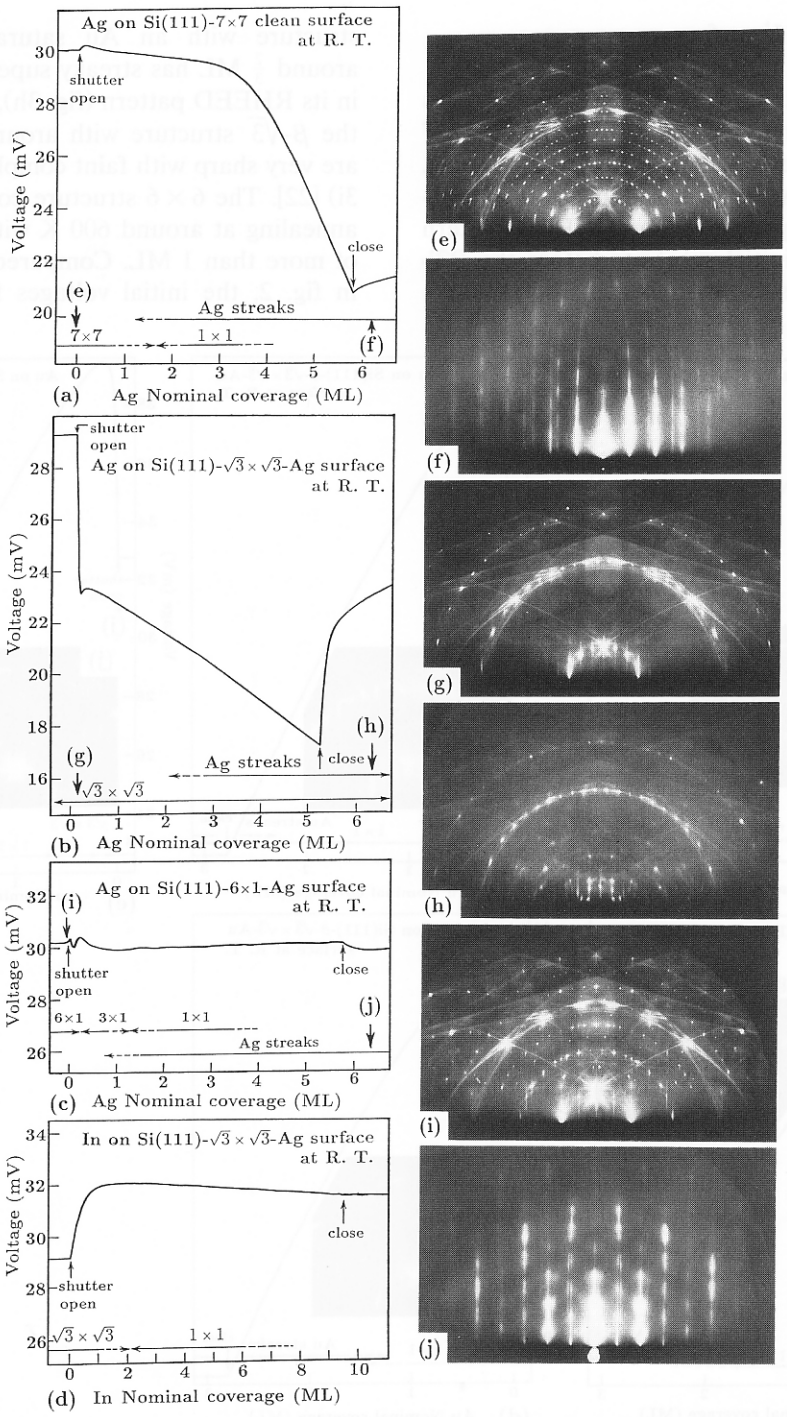

Fig. 2. Resistance changes during the room-temperature Ag depositions onto (a) clean Si(111)-7 × 7, (b) Si(111)-$\sqrt{3} \times \sqrt{3}$-Ag, and (c) Si(111)-6 × 1-Ag surfaces, respectively. (d) Result during In deposition onto Si(111)-$\sqrt{3} \times \sqrt{3}$-Ag surface. RHEED patterns are shown: (e) clean Si(111)-7 × 7, (f) a texture structure after 5.8 ML Ag deposition onto the 7 × 7 surface, (g) $\sqrt{3} \times \sqrt{3}$-Ag substrate before the Ag deposition, (h) after 5.2 ML Ag deposition onto (g), (i) 6 × 1-Ag surface before the Ag deposition, and (j) after 5.6 ML Ag deposition onto (i).

3.2. Au on a Si(111) surface

Fig. 3 shows the results for Au depositions (rate: 0.21 ML/min) at RT onto a clean 7×7 (fig. 3a), 5×2-Au (fig. 3b), α-$\sqrt{3} \times \sqrt{3}$-Au (fig. 3c), β-$\sqrt{3} \times \sqrt{3}$-Au (fig. 3d), and 6×6-Au surfaces (fig. 3e), respectively. The RHEED pattern taken from each initial substrate before the RT-deposition of Au is shown in figs. 3f–3j. The α-$\sqrt{3}$ structure with an Au saturation coverage of around $\frac{2}{3}$ ML has streaky superlattice reflections in its RHEED pattern (fig. 3h), while the spots of the β-$\sqrt{3}$ structure with around 1 ML coverage are very sharp with faint complicated streaks (fig. 3i) [22]. The 6×6 structure could be built up by annealing at around 600 K with an Au coverage of more than 1 ML. Compared with the Ag case in fig. 2, the initial voltages for each measure-

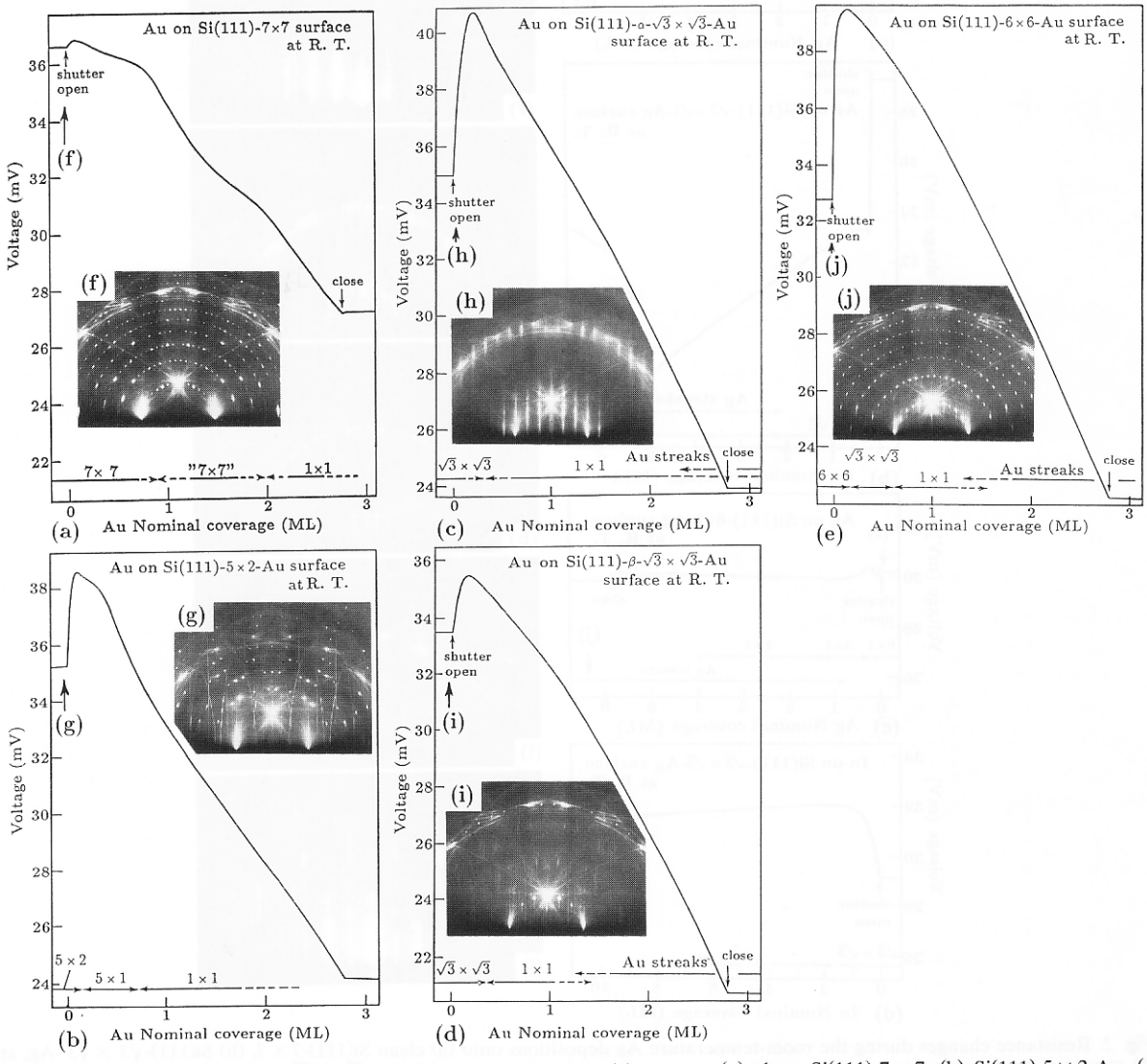

Fig. 3. Resistance changes during the room-temperature Au depositions onto (a) clean Si(111)-7×7, (b) Si(111)-5×2-Au, (c) Si(111)-α-$\sqrt{3} \times \sqrt{3}$-Au, (d) Si(111)-β-$\sqrt{3} \times \sqrt{3}$-Au, and (e) Si(111)-6×6-An surfaces, respectively. RHEED patterns before the Au depositions are shown as insets: (f) clean Si(111)-7×7, (g) 5×2-Au, (h) α-$\sqrt{3} \times \sqrt{3}$-Au, (i) β-$\sqrt{3} \times \sqrt{3}$-Au, and (j) 6×6-Au structures, respectively.

ment before deposition were slightly scattered from one measurement run to another, probably because of interdiffusion of deposited Au during heat treatments.

The resistance in fig. 3a does not show a significant change at the initial deposition, except for a slight increase at the beginning, similar to the Ag case (fig. 2a). The subsequent decrease in resistance temporarily slows down around 2 ML Au coverage, during which the 7×7 pattern seems different from the clean one (fig. 3f) in the intensity distribution of superlattice spots. On the other hand, after preparing the 5×2-Au structure (fig. 3g) at 770 K by Au deposition of ~ 0.5 ML [23–27], the substrate was cooled down to RT, and then the resistance measurement with Au deposition was performed (fig. 3b). The remarkable feature in this case is an abrupt large increase at the beginning. The maximum resistance in this change corresponded to a minor change in the RHEED pattern; the half-order streaks in the 5×2 pattern (fig. 3g) disappeared to convert to a 5×1 structure. Similar changes in resistance were observed for other Au-induced-superstructure substrates as shown in figs. 3c–3e. But the magnitudes of the initial raises in resistance were different depending on the initial surface structures; the resistance most greatly raised for the case of 6×6-Au surface, during which the RHEED pattern converted from 6×6 to $\sqrt{3} \times \sqrt{3}$. The final RHEED patterns with 2.8 ML Au deposition in all cases were almost the same faint 1×1, irrespective of different starting surface structures, which contrasts with the Ag case in fig. 2. We did not observe a recovery change in resistance after the deposition was stopped, such as in fig. 2b.

3.3. Interruption of deposition

Fig. 4 shows the resistance changes during cycles of metal depositions and their interruptions. In the case of Ag deposition at RT onto the $\sqrt{3} \times \sqrt{3}$-Ag surface (fig. 4a), steep decreases and raises in resistance were repeatedly observed at opening and closing the evaporator shutter, respectively. In the case of Au deposition at RT

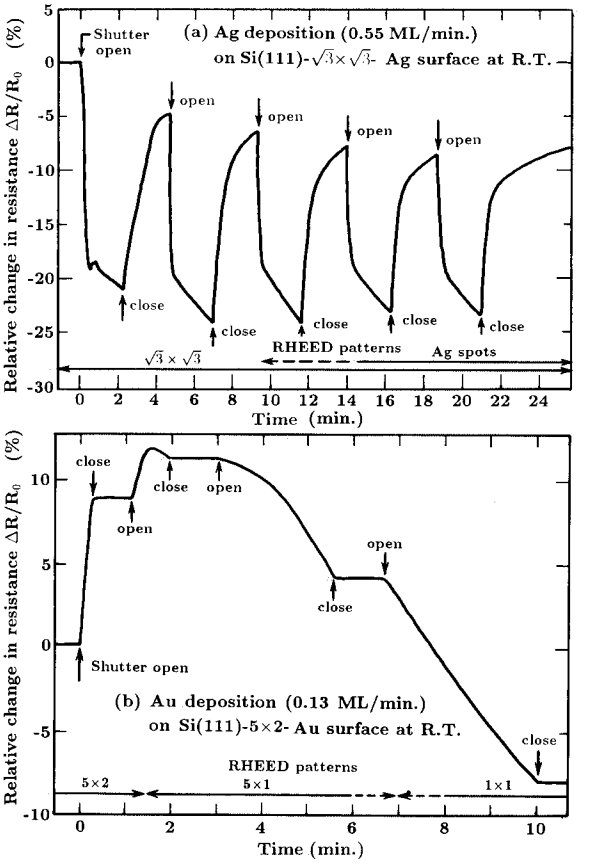

Fig. 4. Resistance changes during the cycles of room-temperature metal depositions and their interruptions; (a) Ag deposition onto Si(111)-$\sqrt{3} \times \sqrt{3}$-Ag, and (b) Au deposition onto Si(111)-5×2-Au surfaces, respectively.

onto the 5×2-Au surface, on the other hand, the resistance followed a similar change as in fig. 3b during the deposition periods, but it remained constant during the interruption periods. This difference between Ag and Au cases during the interruption periods may be attributed to surface diffusion and nucleation of deposited adatoms, as discussed in the next section.

4. Discussion

In both cases of Ag and Au, there were remarkable differences between resistance changes during metal depositions onto the clean 7×7 surface and onto the metal-induced superstruc-

ture surfaces. In particular, the resistance changes at low metal coverages (less than 1 ML) were noticeable; a steep decrease for the Ag case (fig. 2b) and steep raises for the Au cases (figs. 3b–3e) were observed for the metal-induced superstructure surfaces, while no significant changes were observed for the 7×7 surface. In the region of such an initial stage of deposition, any electrical conductions through the deposited metal films are not considered to be enough to contribute to the measured resistance changes. It is natural, then, to expect that the conduction through the underlying substrate is modulated by metal-atom adsorptions. It has been well understood [1,2,9–12] that adsorptions of foreign materials such as gases and alkali-metals onto semiconductor surfaces cause changes in surface conductivity because of band bending changes at the surfaces due to the donor- or acceptor-like actions of the adsorbates. That is, the Fermi level at the surface shifts and the band bending changes upon adsorption of metal atoms, resulting in a change in carrier concentration in the space-charge layer. Although the change in surface conductance is composed of the product of a mobility and an excess carrier concentration, the mobility change is probably not of prime importance in our case.

We can, therefore, explain the structure-dependent variations in the resistance changes mentioned in the previous section as follows. The Fermi level at the Si(111)-7×7 surface has been proved to be pinned at the middle of the band gap by an intrinsic surface state, a metallic state, originating from the dangling-bond state on the adatoms [28] of the dimer–adatom–stacking-fault structure [29]. The Fermi level is so strongly pinned at the state that the band bending scarcely changes with adsorption of metal atoms, resulting in small changes in conductance at the beginning of metal depositions onto the 7×7 surface (figs. 2a and 3a).

Taking into account the fact that the Si(111)-$\sqrt{3} \times \sqrt{3}$-Ag surface is "semiconducting" [30,31], on the other hand, the Fermi level at the surface is expected to much more easily shift with the subsequent Ag adsorption. Since the Ag adatoms are considered to act as donors, the band will bend downwards to increase the concentration of conduction electrons in the space-charge layer. A very small amount of Ag adatoms is enough to cause such variation, resulting in an abrupt decrease in resistance at the beginning of deposition in fig. 2b.

The resistance change for In adsorption onto the same $\sqrt{3} \times \sqrt{3}$-Ag surface (fig. 2d) is similarly understood. But, in this case, the bands are made to bend slightly upwards to decrease the carrier concentration because of acceptor-like action of In adatoms. Since the In adatoms destroy the $\sqrt{3}$-Ag structure, contrasting to Ag adatoms, the surface states will significantly change with the structural change to produce acceptor-like states. Ag (group I) and In (group III) adatoms are, in this way, quite different in electronic actions on the $\sqrt{3}$-Ag surface.

Since Ag adsorption up to 5.6 ML coverage onto the 6×1-Ag surface scarcely raise significant change in resistance (fig. 2c), the Fermi level at this surface is also considered to be strongly pinned. Because the saturation Ag coverage for the 6×1 (or 3×1) structure is believed to be $\frac{1}{3}$ ML [18,32] and an Ag atom has a single valence electron, the dangling bonds on the Si(111) surface are not completely terminated, resulting in a "metallic surface". This is the origin of the strong pinning of the Fermi level (stronger than on the clean 7×7 surface).

Ultraviolet photoemission spectroscopy data [33] indicate that the bands at the Au-induced surface structures, 5×2, α-$\sqrt{3} \times \sqrt{3}$, β-$\sqrt{3} \times \sqrt{3}$, and 6×6 surfaces bend upwards strongly enough to create a p-type inversion layer due to acceptor-like surface states. This may be related to the larger electronegativity of Au than those of Si and Ag. Then, the great increases in resistance upon Au adsorption in figs. 3b–3e are understood as follows. The "pinning forces" for the Fermi level are again weak on these surfaces, so that Au adsorptions onto these surfaces easily make the bands bend downwards because of the donor-like action of the Au adatoms. This means a decrease of the hole concentration in the space-charge region. After reaching the minimum surface conductance of a depletion layer, the surface will convert to an n-type accumulation layer and turn to a decrease in resistance for the

duration of the deposition. The carrier concentration and its sign, holes or electrons, can be determined as a change in the Hall voltage. The in situ measurements of the Hall effect combined with RHEED observation and the conductance measurement are now carried out to prove the above-mentioned variations in band bending, and their results will be soon published elsewhere.

Kono et al. [34] reported core-level shifts in X-ray photoemission spectra indicating an upward bending of the bands at the Si(111)-$\sqrt{3} \times \sqrt{3}$-Ag surface to create an inversion layer. Combining their result with our conductance measurements, the subsequently deposited Ag adatoms on the $\sqrt{3}$-Ag surface will have to act as an acceptor to bend the bands further upwards in order to explain the steep decrease in resistance at the beginning of Ag deposition onto the $\sqrt{3}$-Ag surface (fig. 2b). Furthermore, we will have to assume a donor-like action of In adatoms on the $\sqrt{3}$-Ag surface for explaining the steep raise in resistance in fig. 2d. It seems unlikely, however, that these conclusions are consistent with simple expectations that Ag, a noble metal of group I, will donate an electron and In, an element of group III, will accept an electron. It is obvious, of course, that the charge transfers in these metal–Si systems are still open questions for further investigations, theoretically as well as experimentally.

With increase of the metal coverages, the donor- or acceptor-like actions of the metal adatoms mentioned so far will change because of mutual interactions between the adatoms. That is, the charge transfer between the adsorbates and the substrate will change with aggregation of isolated adatoms on the surface. So the above-mentioned simple picture of band bending and "surface doping" effect by adatoms will have to be modified near 1 ML coverage.

We interpret the recovery changes after the deposition off in the case of Ag on Si(111)-$\sqrt{3} \times \sqrt{3}$-Ag surface (figs. 2b and 4a) as the change in degree of the donor-like action of Ag adatoms due to their mutual interactions. Due to high surface diffusivity of Ag atoms on the $\sqrt{3}$-Ag surface, the deposited Ag monomers will congregate into 3D nuclei as shown in the RHEED pattern (fig. 2h), resulting in decrease in charge transfer into the substrate, and the resistance change recovers. The 3D Ag islands on the $\sqrt{3}$-Ag surface scarcely seem to contribute to the surface conductance. In the case of Au on Si(111)-5 × 2-Au surface, the resistance remained constant during the interruptions of deposition (fig. 4b), suggesting no significant nucleation of deposited Au adatoms, in contrast to the Ag case. Another important factor to be considered for explaining the difference in resistance changes during the interruption periods between Ag and Au (fig. 4) may be their reactivity with Si. The Ag–Si(111) interface is known to be nearly abrupt without intermixing of the components [35,36], while Au forms interfaces which are highly intermixed [37].

When the metal coverage further increases, the conduction through the grown metal film may dominate the resistance changes, the effect of which strongly depends on the epitaxial growth mechanisms. The rate of decrease in resistance during Ag deposition in the thicker coverage region (more than 3 ML) was quite different between figs. 2a and 2b. This seems to support a simple expectation that 2D Ag islands on the surface (fig. 2a) more easily create percolation paths than 3D Ag nuclei (fig. 2b). The thick Au films, on the other hand, seem similar in structure, irrespective of the initial substrate surface, resulting in almost equal rates of decrease in resistance with Au coverage (figs. 3a–3e).

5. Conclusions

We have found the strong dependence of changes in Si(111) surface conductance during metal depositions upon the substrate–surface structures. This phenomenon is mainly understood with changes in space-charge layer caused by "surface doping" effects of metal adatoms. The variations in the space-charge layer of thickness of order of 100 nm sensitively depend on the structures of several topmost atomic layers of the surface. Further investigations such as Hall coefficient measurements and photoemission spectroscopy, as well as theoretical calculations, are needed to fully understand the mechanisms of changes in electrical characteristics of the sur-

faces. In situ measurements like the present study will not only provide valuable insight into the fundamental understanding of surface and interface phenomena such as metallization of surfaces and Schottky-barrier formation, but will also lead to industrial applications.

Acknowledgement

The present study was supported in part by a Grant-in-Aid from the Ministry of Education, Science and Culture of Japan, and also by the Murata Science Foundation.

References

[1] A. Many, Y. Goldstein and N.B. Grover, Semiconductor Surfaces (North-Holland, Amsterdam, 1965).
[2] D.R. Frankl, Electrical Properties of Semiconductor Surfaces (Pergamon, Oxford, 1967).
[3] I.P. Batra, Ed., Metallization and Metal–Semiconductor Interfaces (Plenum, New York, 1988).
[4] For example: Surf. Sci. 73 (1978); 98 (1980); 113 (1982); 142 (1984); 170 (1986); 196 (1988); 229 (1990).
[5] P.K. Larson and P.J. Dobson, Eds., Reflection High-Energy Electron Diffraction and Reflection Electron Imaging of Surfaces (Plenum, New York, 1988).
[6] L.J. Brillson, Surf. Sci. Rep. 2 (1982) 123.
[7] R.T. Tung, Phys. Rev. Lett. 52 (1984) 461.
[8] D.R. Heslinga, H.H. Weitering, D.P. van der Werf, T.M. Klapwijk and T. Hibma, Phys. Rev. Lett. 64 (1990) 1589.
[9] G. Allen and G.W. Gobell, Phys. Rev. 144 (1966) 558.
[10] W. Mönch, Phys. Status Solidi 40 (1970) 257.
[11] L. He and H. Yasunaga, Jpn. J. Appl. Phys. 24 (1985) 928.
[12] L. Surnev and M. Tikhov, Surf. Sci. 85 (1979) 413.
[13] J.E. Demuth and B.N.J. Persson, J. Vac. Sci. Technol. B 2 (1984) 384; Phys. Rev. Lett. 54 (1985) 584.
[14] B.N.J. Persson and J.E. Demuth, Solid State Commun. 54 (1985) 425; Phys. Rev. B 31 (1985) 1856.
[15] M. Jałochowski and E. Bauer, Phys. Rev. B 37 (1988) 8622; 38 (1988) 5272; Surf. Sci. 213 (1989) 556.
[16] S. Hasegawa and S. Ino, Phys. Rev. Lett. 68 (1992) 1192.
[17] Y. Gotoh and S. Ino, Jpn. J. Appl. Phys. 17 (1978) 2097; Thin Solid Films 109 (1983) 255; J. Cryst. Growth 56 (1982) 498.
[18] S. Hasegawa, H. Daimon and S. Ino, Surf. Sci. 186 (1987) 138.
[19] M. Katayama, R.S. Williams, M. Kato, E. Nomura and M. Aono, Phys. Rev. Lett. 66 (1991) 2762.
[20] T. Takahashi, S. Nakatani, N. Okamoto, T. Ishikawa and S. Kikuta, Jpn. J. Appl. Phys. 27 (1988) L753.
[21] G. LeLay, G. Quentel, J.P. Faurie and A. Masson, Thin Solid Films 35 (1976) 273.
[22] S. Ino, in: Reflection High-Energy Electron Diffraction and Reflection Electron Imaging of Surfaces, Eds. P.K. Larson and P.J. Dobson (Plenum, New York, 1988) p. 3; Jpn. J. Appl. Phys. 16 (1977) 891.
[23] H. Daimon, C. Chung, S. Ino and Y. Watanabe, Surf. Sci. 235 (1990) 142.
[24] S. Takahashi, Y. Tanishiro and K. Takayanagi, Surf. Sci. 242 (1991) 73.
[25] Y. Tanishiro, K. Yagi and K. Takayanagi, Surf. Sci. 234 (1990) 37.
[26] A.A. Baski, J. Nogami and C.F. Quate, Phys. Rev. B 41 (1990) 247.
[27] E. Bauer, Surf. Sci. Lett. 250 (1991) L379.
[28] R.J. Hamers, R.M. Tromp and J.E. Demuth, Phys. Rev. Lett. 56 (1986) 1972.
[29] K. Takayanagi, Y. Tanishiro, M. Takahashi and S. Takahashi, J. Vac. Sci. Technol. A 3 (1985) 1502; Surf. Sci. 164 (1985) 367.
[30] T. Yokotsuka, S. Kono, S. Suzuki and T. Sagawa, Surf. Sci. 127 (1983) 35.
[31] J.M. Nicholls, F. Salvan and B. Reihl, Phys. Rev. B 34 (1986) 2945.
[32] G. LeLay, M. Manneville and R. Kern, Surf. Sci. 72 (1978) 405.
[33] H. Daimon, Y. Tezuka and S. Ino, to be published.
[34] S. Kono, K. Higashiyama, T. Kinoshita, T. Miyahara, H. Kato, H. Ohsawa, Y. Enta, F. Maeda and Y. Yaegashi, Phys. Rev. Lett. 58 (1987) 1555.
[35] M. Saitoh, F. Shoji, K. Oura and T. Hanawa, Jpn. J. Appl. Phys. 19 (1980) L421; Surf. Sci. 112 (1981) 306.
[36] J. Stöhr, R. Jaeger, G. Rossi, T. Kendelewicz and I. Lindau, Surf. Sci. 134 (1984) 813.
[37] A. Hiraki, Surf. Sci. Rep. 3 (1984) 357.